HHS Public Access

Author manuscript

Biochem Biophys Res Commun. Author manuscript; available in PMC 2015 December 02.

Published in final edited form as:

Biochem Biophys Res Commun. 2010 August 20; 399(2): 129–132. doi:10.1016/j.bbrc.2010.07.022.

RANKL-RANK signaling regulates expression of Xenotropic Polytropic Virus Receptor (XPR1) in osteoclasts

Parul Sharma[*,#], **Somying Patntirapong**[#,@], **Steven Hann**[#], and **Peter V. Hauschka**[#]

[#]Department of Orthopedic Surgery, Children's Hospital, Boston. MA-02115 [@]Faculty of Dentistry, Thammasat University, Patumthani, 12121. Thailand

Abstract

Formation of multinucleated bone-resorbing osteoclasts results from activation of the Receptor activated NF-κB ligand (RANKL)-receptor activated NF-κB (RANK) signaling pathway in primary bone marrow macrophages and a macrophage cell line (RAW 264.7). Osteoclasts, through bone remodeling, are key participants in the homeostatic regulation of calcium and phosphate levels within the body. Microarray analysis using Gene Expression Dynamic Inspector (GEDI) clustering software indicated that osteoclast differentiation is correlated with an increase in Xenotropic and Polytropic Virus Receptor 1 (XPR1) mRNA transcripts. XPR1 is a receptor of the xenotropic and polytropic murine leukemia virus and homolog of yeast Syg1 and plant Pi transporter PHO1. Quantitative PCR was used to validate the up-regulation of XPR1 message following RANKL stimulation in both primary bone marrow cells and a macrophage cell line. Immunostaining for the XPR1 protein showed that there is translocation of XPR1 to the membranes of the sealing zone in mature osteoclasts. This study is the first to demonstrate that the expression of retro-viral receptor, XPR1, is regulated by RANKL-RANK signaling.

Introduction

RANKL-RANK signaling is important for differentiation of osteoclasts (1, 2). We identified XPR1, a syg 1 and plant PHO1 homolog (3), as one of the genes within a cluster of gene transcripts up-regulated during osteoclast differentiation. Three independent groups identified xenotropic and polytropic virus receptor (XPR1) as the murine leukemia virus (MLV) receptor(4-7). Murine leukemia viruses are gamma-retro viruses that have been linked in varying degrees to development of hematopoietic neoplasia, osteopetrosis and osteomas in mice and prostate cancer in humans(8). A study by Schmidt *et al.*(9) has shown

[*]Corresponding author: Parul Sharma, Phone: 6179192953, parulsd@hotmail.com, Mailing address: Room 1010 Enders Building, Department of Orthopedic Surgery, Children's Hospital, Boston, 320 Longwood Ave, Boston, MA-02115.

Authorship contributions: PS designed and implemented the experiments and contributed in writing the manuscript. PVH and SH helped in design of experiments and contributed in writing the manuscript. SP helped in the design and implementation of the experiments.

Conflict of interest: The authors declare they have no conflicting interests.

that MLV induced osteopetrosis could be independent of lymphomagenesis and could reside either in osteoblasts or osteoclasts(8).

To elucidate the primary infection site of the MLVs in mouse, Okimoto and Fan(10) used a replication deficient Moloney MLV vector that expressed beta-galactosidase. Positive staining, indicating that viral beta-galactosidase was translated and expressed, was limited to osteoclasts after a peritoneal injection of this replication deficient MLV in mice. The authors suggested that because the viral vector could not diffuse from the peritoneal cavity to the bone, circulating mononuclear osteoclast precursors were the most probable primary site of infection for MLVs and must also express the receptor for this replication deficient retroviral vector (10). This is in keeping with an independent study by Faust et al. that indicated the presence of committed osteoclast precursors amongst peripheral blood mononuclear cells (11).

We show that XPR1 is expressed at low levels in the RAW264.7 macrophage cell line and primary bone marrow cells, and persists under standard culture conditions. An increase in XPR1 transcript was noted by microarray hybridization and QRT-PCR, in response to RANKL-RANK signaling and osteoclastogenesis. This up-regulation of XPR1 transcript in response to RANKL was observed in both primary bone marrow cells and RAW264.7 cells. By immunostaining we show that XPR1 is present in the cytoplasm of mononuclear osteoclast precursors and translocates to the membranes of the mature multinucleated osteoclasts.

Materials and methods

Primary mouse bone marrow cells

Bone marrow cells were obtained from 3 week old C57Bl6 mice carrying the SMAEGFP transgene as described in earlier studies (12). Cell suspensions were plated at 5×10^4 cells/well in 96-well plates in α-MEM (Invitrogen, Carlsbad) containing 10% FBS (Atlanta Biologicals), 100u/ml of penicillin/streptomycin (Sigma) and supplemented with 20 ng/ml macrophage colony stimulating factor (M-CSF) and 50 ng/ml RANKLon day 0 and day 3 to induce osteoclast differntiation.

RAW 264.7 cells (ATCC), a mouse monocyte/macrophage cell line, were plated at 2.5×10^4 cells/well in 96-well plates in α-MEM+10% FBS+100u/ml of penicillin/streptomycin. In order to induce osteoclast differentiation, the medium was supplemented with 50 ng/ml of RANKL. All cells were cultured at 37 °C in a humidified atmosphere containing 5% CO_2 in air. Cells were fixed on day 5 for microscopy.

Immunostaining was performed with primary anti-XPR1 and anti-CTSK antibodies (Biovision and Santa Cruz Biotechnology), and Alexa 488 or Alexa 568 labeled secondary donkey anti-goat, anti-rabbit or anti-mouse (Invitrogen), as appropriate. Hoechst 33342 (Immunochemistry LLC), FITC-phalloidin (Invitrogen) and TRAP activity (Sigma) staining were performed according to the manufacturer's protocols.

Gene Expression Dynamic Inspector (GEDI) analysis

RANKL was added twice to RAW 264.7 cells (Day 0, 3) and total RNA was isolated on days 1, 2, 4, & 5 for transcriptome analysis with Affymetrix microarray chips. The normalized data were filtered to include 12,488 gene transcripts (p value <0.05). These microarray data were then analyzed with GEDI, a "gestalt" program that clusters genes into visual patterns (13). The URL for downloading the free GEDI program is www.childrenshospital.org/research/ingber/GEDI/gedihome.htm

Results and discussion

Mononuclear osteoclast precursors differentiate in response to RANKL-RANK signaling, fusing to form multinuclear osteoclasts and upregulating expression of proteins associated with bone resorption, cathepsin K (CTSK) and tartrate resistant acid phosphatase (TRAP). We used Affymetrix Microarray chips to measure temporal changes in the transcriptome of RAW 264.7 cells treated with RANKL (Geo NCBI accession number GSE21639). This yielded a pool of ∼12,488 transcripts that were significantly expressed above background ($p<0.05$). This pool of genes was further analyzed by GEDI program that grouped them into three distinct clusters. We designated one 471 gene cluster as the differentiation cluster. It included genes that are known to be upregulated during osteoclast differentiation such as CTSK (267 ± 160 fold) and TRAP, (303 ± 74 fold) and others that have not previously been linked to osteoclastogenesis. XPR1 was one of the new upregulated genes identified within this differentiation cluster (12.4 ± 2.6 fold) (Figure 1B). To exclude the possibility that the observed upregulation of XPR1 message was an artifact of the cell line, we analyzed the transcriptomes of primary bone marrow macrophages that were treated with RANKL and M-CSF (n=4) or M-CSF only (n=2) for five days. This experiment used an Illumina MouseRef-6 BeadChip instead of the Affymetrix microarray chip to rule out any microarray method bias. Again, a significant up-regulation (∼10 fold) of the XPR1 transcript was observed in RANKL-treated primary cells (figure 1C).

We used quantitative real-time PCR (QRT-PCR) to examine XPR1 transcription changes in RAW 264.7. This confirmed an up-regulation of the XPR1 transcript (30 ±12 fold) in RANKL-treated cells. The positive template control, TRAP, an established biomarker of osteoclasts, was also up-regulated 70 fold (± 30) (Figure 1D).

Osteoclast differentiation is characterized by the formation of large, multinucleated osteoclasts with upregulated expression of CTSK(14) and TRAP (15). Bright field microscopy (Figure 2A) shows large multinucleated mature osteoclasts (blue arrows, >5 nuclei) that are TRAP positive (black), as well as mononuclear TRAP positive immature osteoclasts (white arrows). The bright field image (Figure 2A) is a grayscale image wherein the intensity of the black TRAP staining reflects the expression of TRAP within the cell. Immunofluorescence in the same field of view shows mature osteoclasts (blue arrows) expressing both CTSK (red, Figure 2B) and TRAP (black, Figure 2A), but not in identical cytoplasmic locations. Immunostaining for XPR1 (Figure 2C) labels the TRAP / CTSK positive osteoclasts (Figure 2D). In a higher magnification view of the inset in Figure 2A (Figures 2E-H) we observed positive XPR1 immunostaining in the peri-nuclear cytoplasm (white arrows) of both mononuclear TRAP positive cells and mature osteoclasts (Figure 2D

and 2H). A mature osteoclast (blue arrow) expressing both TRAP (Figure 2E) and CTSK (Figure 2F) is also clearly seen to express XPR1 (Figure 2G) in the peripheral membrane and membranous extensions (red arrows). In contrast to XPR1, CTSK and TRAP staining is cytoplasmic in both immature and mature osteoclasts, suggesting that XPR1 distribution is dependent on the stage of osteoclast differentiation.

Osteoclasts are dynamic cells with their cytoskeletons forming F-actin rich sealing zones and podosomes (16). These two types of structures in osteoclasts are important for both motility and compartmentalization of the region of bone to be resorbed. Upon mature osteoclast formation, transporters such as vacuolar H(+)-ATPases (V-ATPases) are expressed (Figure1A) and transported from cytosolic compartments to these actin rich zones(17). We observed that XPR1 and F-actin proteins co-localize in the sealing zone membranes of multinucleated but not mononuclear osteoclasts, suggesting a distinct role for XPR1 in these cells (data not shown). XPR1, has a yeast homolog Syg1 and a plant homolog Pho1, which are linked to regulation of alpha G_s protein signaling and phosphate sensing/ transport respectively; both are membrane-restricted functions. All six identified receptors of gamma family retroviruses have been shown to be transporters(10).

The literature is ambiguous regarding virus-osteoclast interactions; for example the localization of virus like particles in osteoclasts from patients with Paget's disease (18-21). Expression of MLV derived beta-galactosidase has been reported in murine bone marrow osteoclasts (10) and XPR1 expression in fibroblasts makes these non-permissive cells susceptible to retroviral infection (4). Unique variations in the viral binding sites on XPR1(22, 23) are reported to influence the host range of MLVs. A polymorphic nature has been suggested for XPR1 that would allow it to be more permissive to viral infections in non-murine species (5, 7, 24).

This study links RANKL-RANK induction of osteoclastogenesis with the regulation of expression of the viral infectivity factor XPR1. With the recent detection of expression of a XMRV, a virus capable of binding XPR1 receptor, in human prostate cancer patients(25), and reports of viral particles in osteoclasts from Paget's disease patients(5, 7, 24) our findings suggest new mechanisms and possible targets in osteoclast biology and in cancer.

Acknowledgments

The research was supported by Department of Orthopedic Surgery funds (PVH), NRSA T32 Grant (PS). We acknowledge the support of Microarray core facilities at Harvard and Children's Hospital Boston in collection and normalization of the microarray data. We thank Dr. Sui Huang for helpful suggestions on GEDI analysis of microarray data.

References

1. Lacey DL, Timms E, Tan HL, Kelley MJ, Dunstan CR, Burgess T, Elliott R, Colombero A, Elliott G, Scully S, Hsu H, Sullivan J, Hawkins N, Davy E, Capparelli C, Eli A, Qian YX, Kaufman S, Sarosi I, Shalhoub V, Senaldi G, Guo J, Delaney J, Boyle WJ. Cell. 1998; 93:165–176. [PubMed: 9568710]
2. Li J, Sarosi I, Yan XQ, Morony S, Capparelli C, Tan HL, McCabe S, Elliott R, Scully S, Van G, Kaufman S, Juan SC, Sun Y, Tarpley J, Martin L, Christensen K, McCabe J, Kostenuik P, Hsu H,

Fletcher F, Dunstan CR, Lacey DL, Boyle WJ. Proc Natl Acad Sci U S A. 2000; 97:1566–1571. [PubMed: 10677500]

3. Hamburger D, Rezzonico E, MacDonald-Comber Petetot J, Somerville C, Poirier Y. Plant Cell. 2002; 14:889–902. [PubMed: 11971143]
4. Battini JL, Rasko JE, Miller AD. Proc Natl Acad Sci U S A. 1999; 96:1385–1390. [PubMed: 9990033]
5. Levy JA. Proc Natl Acad Sci U S A. 1999; 96:802–804. [PubMed: 9927648]
6. Marin M, Tailor CS, Nouri A, Kozak SL, Kabat D. J Virol. 1999; 73:9362–9368. [PubMed: 10516044]
7. Tailor CS, Nouri A, Lee CG, Kozak C, Kabat D. Proc Natl Acad Sci U S A. 1999; 96:927–932. [PubMed: 9927670]
8. Ethelberg S, Tzschaschel BD, Luz A, Diaz-Cano SJ, Pedersen FS, Schmidt J. J Virol. 1999; 73:10406–10415. [PubMed: 10559359]
9. Schmidt J, Lumniczky K, Tzschaschel BD, Guenther HL, Luz A, Riemann S, Gimbel W, Erfle V, Erben RG. Am J Pathol. 1999; 155:557–570. [PubMed: 10433948]
10. Okimoto MA, Fan H. J Virol. 1999; 73:1617–1623. [PubMed: 9882368]
11. Faust J, Lacey DL, Hunt P, Burgess TL, Scully S, Van G, Eli A, Qian Y, Shalhoub V. J Cell Biochem. 1999; 72:67–80. [PubMed: 10025668]
12. Sharma P, Solomon KR, Hauschka PV. Biotechniques. 2006; 41:539–540. 542. [PubMed: 17140108]
13. Eichler GS, Huang S, Ingber DE. Bioinformatics. 2003; 19:2321–2322. [PubMed: 14630665]
14. Shi GP, Chapman HA, Bhairi SM, DeLeeuw C, Reddy VY, Weiss SJ. FEBS Lett. 1995; 357:129–134. [PubMed: 7805878]
15. Hayman AR, Cox TM. J Bone Miner Res. 2003; 18:1905–1907. [PubMed: 14584904]
16. Kanehisa J, Yamanaka T, Doi S, Turksen K, Heersche JN, Aubin JE, Takeuchi H. Bone. 1990; 11:287–293. [PubMed: 2242294]
17. Holliday LS, Bubb MR, Jiang J, Hurst IR, Zuo J. J Bioenerg Biomembr. 2005; 37:419–423. [PubMed: 16691476]
18. Mozar A, Haren N, Chasseraud M, Louvet L, Maziere C, Wattel A, Mentaverri R, Morliere P, Kamel S, Brazier M, Maziere JC, Massy ZA. J Cell Physiol. 2008; 215:47–54. [PubMed: 17894387]
19. Matthews BG, Afzal MA, Minor PD, Bava U, Callon KE, Pitto RP, Cundy T, Cornish J, Reid IR, Naot D. J Clin Endocrinol Metab. 2008; 93:1398–1401. [PubMed: 18230662]
20. Helfrich MH, Hobson RP, Grabowski PS, Zurbriggen A, Cosby SL, Dickson GR, Fraser WD, Ooi CG, Selby PL, Crisp AJ, Wallace RG, Kahn S, Ralston SH. J Bone Miner Res. 2000; 15:2315–2329. [PubMed: 11127197]
21. Kurihara N, Zhou H, Reddy SV, Garcia Palacios V, Subler MA, Dempster DW, Windle JJ, Roodman GD. J Bone Miner Res. 2006; 21:446–455. [PubMed: 16491293]
22. Yan Y, Knoper RC, Kozak CA. J Virol. 2007; 81:10550–10557. [PubMed: 17634227]
23. Yan Y, Liu Q, Kozak CA. Retrovirology. 2009; 6:87. [PubMed: 19811656]
24. Yang YL, Guo L, Xu S, Holland CA, Kitamura T, Hunter K, Cunningham JM. Nat Genet. 1999; 21:216–219. [PubMed: 9988277]
25. Fischer N, Hellwinkel O, Schulz C, Chun FK, Huland H, Aepfelbacher M, Schlomm T. J Clin Virol. 2008; 43:277–283. [PubMed: 18823818]

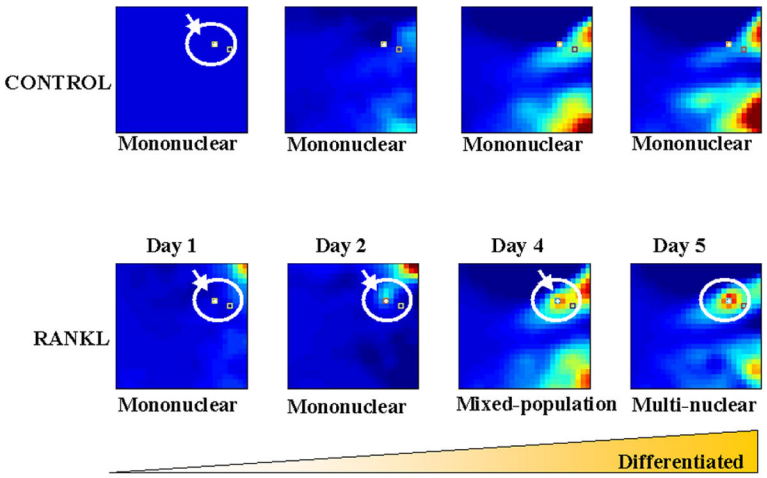

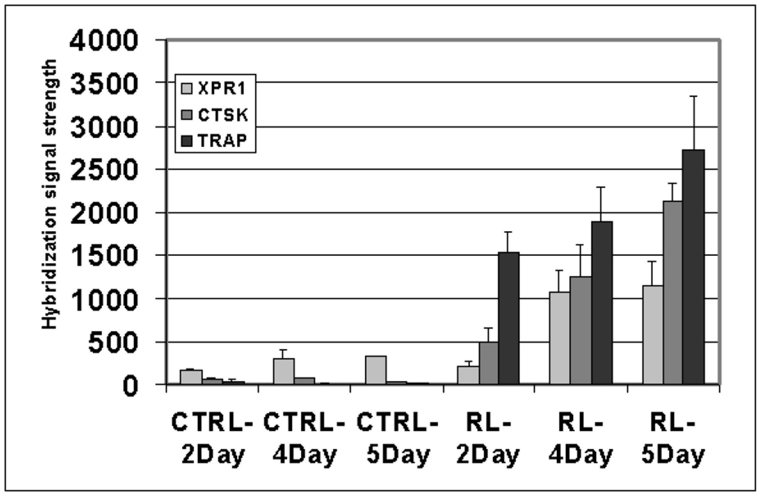

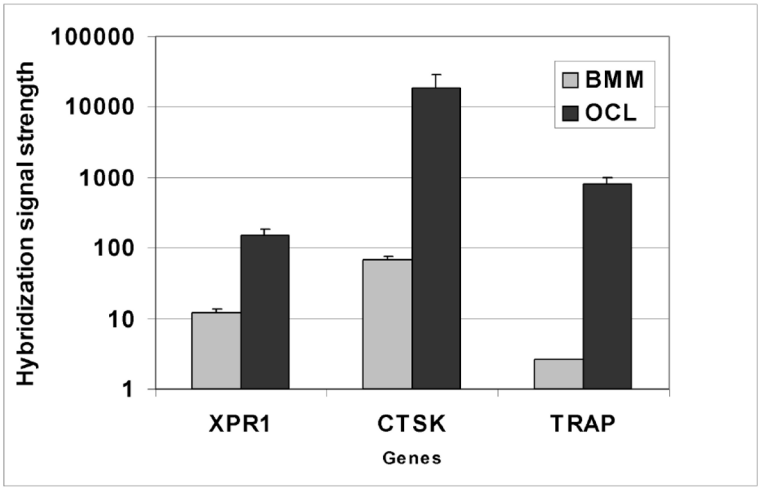

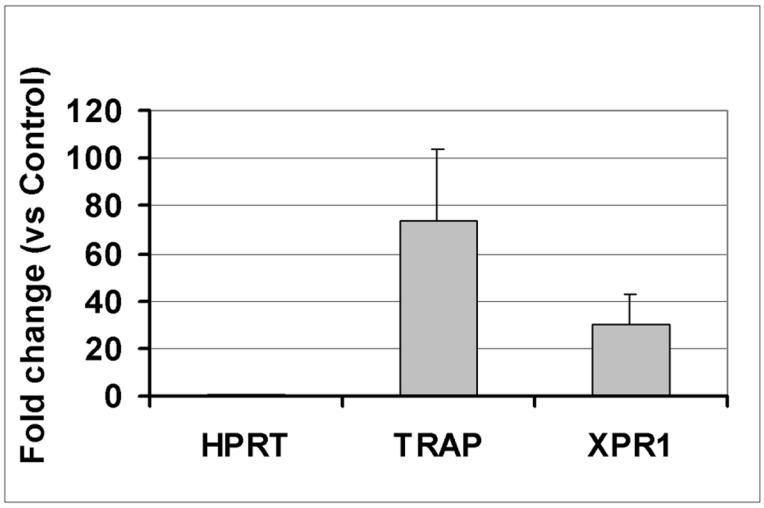

Figure 1.

Regulation of the XPR1 transcript in response to RANKL-RANK signaling: Total RNA was extracted from cultured cells using RNEasy kit (Qiagen, CA) and used for microarray hybridization or preparation of cDNA for QRT-PCR analysis. GEDI analysis was performed on the normalized microarray data of RAW 264.7 (ATCC, Bethesda) cells treated for 5 days with and without RANKL(50ng/ml). The U74av2 mouse Affymetrix chip was used. Microarray data were filtered to include genes that had a significant ($p<0.05$) hybridization signal in at least one sample. The raw GEDI analysis was normalized against day 0 control data for all samples. GEDI analysis provides irreducible information inherent in a cell's transcriptome by providing a visual heat map of the gene expression profile (13). The GEDI profile encompasses all the genes that are provided by the hybridization of the transcripts and distributes them in self-organizing maps. GEDI gave the relative transcriptome signatures of control and RANKL treated RAW cells. The metagene signature of each sample is a 26 × 25 grid of tiles, each of which contains genes that are highly correlated with each other. The tiles are arranged such that each tile is also correlated with the adjacent tiles. The metagene signature tile for each sample is unique to the sample and shows the expression level of the genes after the signal level of the control sample was subtracted from all samples. Red squares indicate genes with higher expression than controls and dark blue squares indicate a reduction in expression levels compared to controls. **1A)**: Representative metagene signatures are shown for temporal changes in the hybridization signal of control (top panel) and RANKL (lower panel) treated cells after normalization with control day 1 samples. The nuclearity of the cells is indicated as mononuclear (undifferentiated) or multinuclear (differentiated). The metagene cluster encircled in white (differentiation) shows changes in the metagene transcriptome signatures of RANKL treated and control cells. The arrow indicates the tiles containing the differentiation cluster of genes including CTSK (white tile), TRAP and XPR1 another outlined tile contains a subunit of a vacuolar ATPase. **1B)**: Microarray data for the RAW 264.7 cell line, showing change in expression levels (signal hybridization strength, y-axis) for XPR1, TRAP and CTSK transcripts after treatment with and without RANKL (days & treatment, x-axis). **1C)**. Comparison of expression levels at 5d(signal hybridization strength, y-axis) of XPR1 transcript in primary bone marrow macrophages (BMM, treated with M-CSF only) or osteoclasts (OCL, treated

with M-CSF + RANKL) with cells from an untreated reference set that included primary bone marrow cells and an osteoblastic cell line. Whole genome expression microarray data was obtained using Illumina MouseRef-6 BeadChips;*p<0.005. **1D)** Quantitative RT-PCR of XPR1 transcript levels (n=2) RANKL treated RAW cells normalized against control RAW cells. XPR1 transcript cDNA template was prepared using oligo dT18 (IDTDNA) and Ready-To-Go™ You-Prime First -strand Beads (GE). QRT-PCR was carried out using Sybr green (ABI) kit to amplify the PCR products using the specified templates on the 7900-HT (ABI) instrument. The values are reported as fold change and error bars denote S.D.. TRAP was used as a positive control for the templates, and all QRT-PCR values were internally normalized to HPRT, a housekeeping gene transcript using the same cDNA template. The primer sequences are given as follows:

XPR1-forward: 5′-TCCACCTACGGAGGACAATC-3′;

XPR1-reverse: 5′-GGAGAAGTGCAGGCAAGAAC-3′;

HPRT-forward: 5′-TCAAGGGCATATCCAACAACAAAC-3′;

HPRT-reverse: 5′- TGGTTCATGGCCAGTTCATA-3′;

TRAP-forward: 5′-GGTCACTGCCTACCTGTGTG-3′;

TRAP-reverse: 5′-ACATAGCCCACACCGTTCTC-3′.

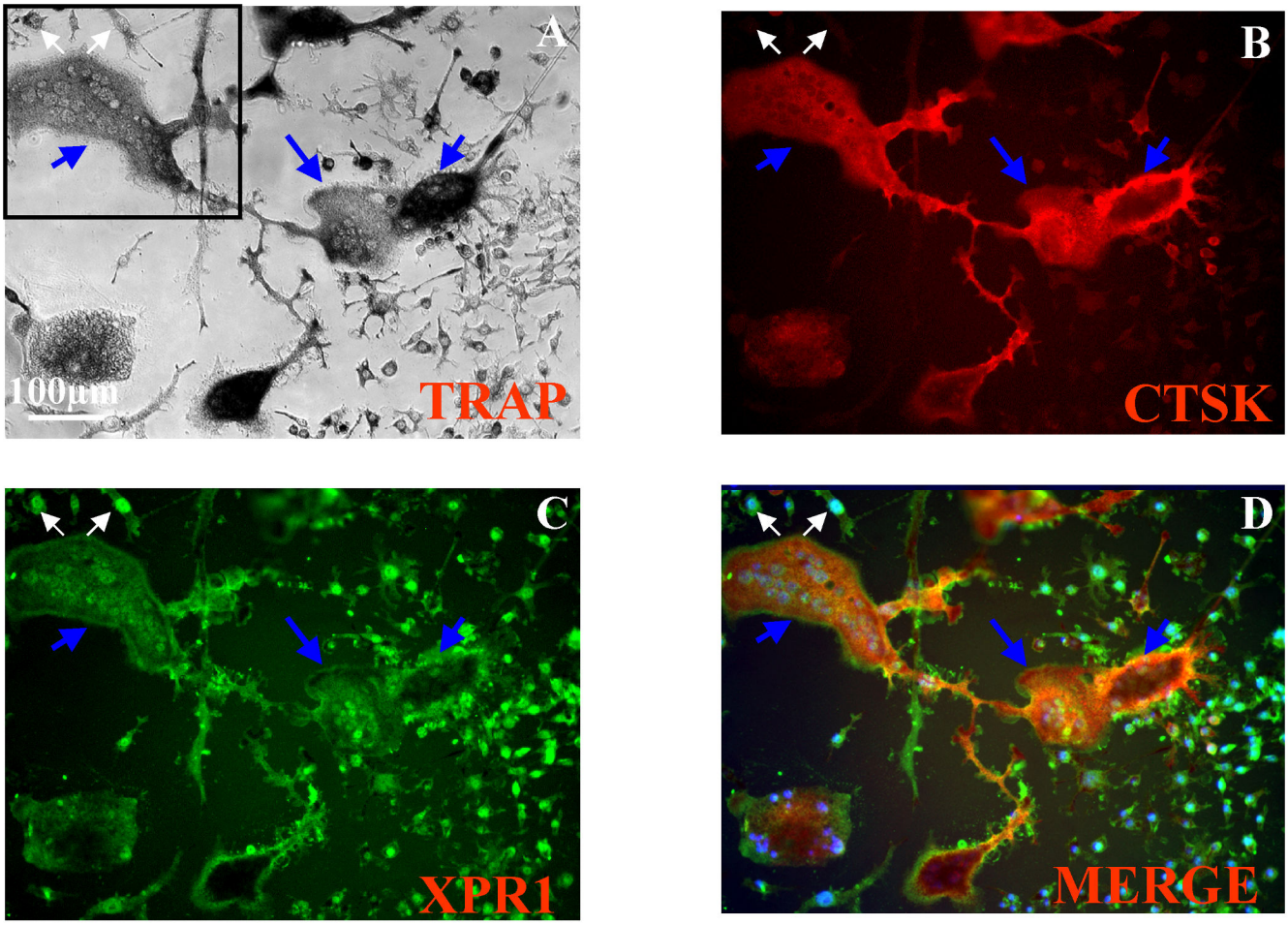

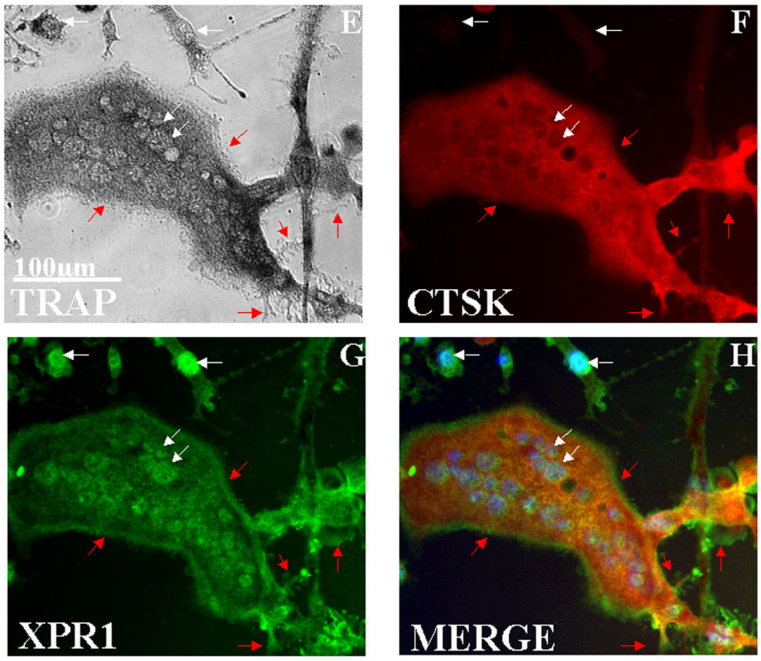

Figure 2.

Expression and localization of XPR1 protein in osteoclasts: A) Multinucleated osteoclasts (blue arrows) and mononuclear pre-osteoclasts (white arrows) are shown to be TRAP positive (black). B) Multinucleated osteoclasts coexpress CTSK (red) and C) XPR1 (green). D) An overlay of TRAP, CTSK and XPR1 staining along with nuclei (blue) shows the distinct distribution of these proteins in the osteoclasts. Orange indicates overlap of the XPR1 and CTSK immunostaining. 2E) The inset in figure 2A is shown at a higher magnification and includes one multinucleated osteoclast and three mononuclear cells that are TRAP positive (grey black) cells. Immunostaining shows the multinucleated osteoclast is strongly positive for 2F) CTSK(red) and 2G) XPR1(green). H) Overlay shows that TRAP, CTSK, and XPR1 have distinct localizations within the nuclei (white arrows) and peripheral membranes and membraneous extensions (red arrows) of the mature osteoclasts. Hoechst 33342 stained nuclei colocalize with XPR1 staining (blue) in both mononuclear and multinuclear osteoclasts. Images were collected on a Nikon TE-2500 fluorescence microscope, and processed using SPOT software and Adobe Photoshop.